

# A Novel Image Denoising Algorithm Based on Riemann-Liouville Definition

Jinrong HU

College of Computer Science, Sichuan University, Chengdu, Sichuan, China

Email: dewhjr@hotmail.com

Yifei PU, Jiliu ZHOU

College of Computer Science, Sichuan University, Chengdu, Sichuan, China

Email: puyifei\_007@163.com, zhoujl@scu.edu.cn

**Abstract**—In this paper, a novel image denoising algorithm named fractional integral image denoising algorithm (FIIDA) is proposed, which based on fractional calculus Riemann-Liouville definition. The structures of  $n \times n$  fractional integral masks of this algorithm on the directions of 135 degrees, 90 degrees, 45 degrees, 0 degrees, 180 degrees, 315 degrees, 270 degrees and 225 degrees are constructed and discussed. The denoising performance of FIIDA is measured using experiments according to subjective and objective standards of visual perception and PSNR values. The simulation results show that the FIIDA's performance is prior to the Gaussian smoothing filter, especially when the noise standard deviation is less than 30.

**Index Terms**—fractional calculus, fractional integral, fractional integral mask, image denoising, Gaussian smoothing filter

## I. INTRODUCTION

Fractional calculus has long history as same as integral calculus and was presented 300 years ago relative to traditional integral calculus. Along with successful application in the research fields of diffusion process, viscoelastic theory and stochastic fractal dynamic, the fractional calculus is applied to the research field of modern signal analysis and processing [1] available at [http://mechatronics.ece.usu.edu/foc/fo\\_sigpro.html](http://mechatronics.ece.usu.edu/foc/fo_sigpro.html). Now, this research field, especially applying it to digital image processing, has obtained some results [2]. On the basis of fractional calculus Grünwald-Letnikov definition, some researchers established the theory of image texture enhancement fractional differentiation operation-based, designed and implemented fractional differentiation filter of digital image [3,4].

As is well known, in existing fractional calculus definition, the fractional differential operation is performed if the order is positive; oppositely, the fractional integral operation is performed if the order is negative. Denoising algorithm is substantially performing an integral calculation for the blocks consisting of image pixels and neighborhood pixels. Otherwise, modern signal analysis and processing is essentially researching

non-linear, non-causal, non-minimum phase system, non-Gaussian, non-steady, non-integer dimension (or fractal) signal and non-white additive noise [5]. Researches show that some fractional operation-based methods are power tools for analyzing and processing said non problems, such as fractional Fourier transform[6,7], fractional wavelet packet transform[8], fractional wavelet spline transform[9], and fractional Brownian motion[10]. These researches show that fractional calculus is also a power tool for analyzing and processing said non problems. In a digital image, the gray values between pixels in neighborhood have great dependency, image signals are highly self-similar, most fractal structures are evolution process (e.g. fractal growing) and final products of evolution (e.g. fracture), and the similar fractal structure in an image is usually featured by edge and texture detail. Meanwhile, fractional calculus is a powerful tool for processing fractal [11,12]. Accordingly, we can think of naturally that whether the fractional calculus theory can be introduced to the digital image with reserving edge and texture detail information when denoising? Thus, this paper aims to introduce fractional calculus to digital image processing, and on the basis of fractional calculus Riemann-Liouville definition, provides a novel fractional integral image denoising algorithm, which is prior to the Gaussian smoothing filter [13], especially when the noise standard deviation is less than 30.

The remainder of this paper is as follows. In section II, we introduce the fractional integral image denoising algorithm (FIIDA), constructing the fractional integral mask on eight directions. In section III, we analyze and discuss the FIIDA by comparative results on test images. Finally, conclusions are drawn in Section IV.

## II. CONSTRUCTION OF FRACTIONAL INTEGRAL MASK

Under the Euclidean measure, except for fractional calculus Grünwald-Letnikov definition, fractional calculus Riemann-Liouville definition also be widely applied and researched. This definition is derived from integer integral definition [2, 14]. For analytic function  $s(x)$  of complex plane, the Cauchy Integral Formula is:

$$\begin{aligned}
 {}_a D_x^{-n} s(x) &\equiv \int_a^x dt_{n-1} \int_a^{x_{n-1}} d_{n-2} \cdots \int_a^{x_1} s(x_0) dx_0 \\
 &= \frac{1}{(n-1)!} \int_a^x (x-\xi)^{n-1} s(\xi) d\xi
 \end{aligned}
 \tag{1}$$

wherein  $n \in \mathbb{Z}^+$  is integral times of  ${}_a D_t^{-n}$ ,  $a, x$  are integral upper and lower limits respectively;  $\Gamma(\cdot)$  is Gamma function and defined as  $\Gamma(n) = \int_0^\infty e^{-t} t^{n-1} dt$ , and  $(n-1)! = \Gamma(n)$ ; Cauchy Integral Formula is directly extended from integer  $n \in \mathbb{Z}^+$  to real number  $\nu$ , and then fractional integral's definition is obtained:

$${}_a D_x^\nu s(x) \equiv \frac{1}{\Gamma(-\nu)} \int_a^x (x-\xi)^{-\nu-1} s(\xi) d\xi \tag{2}$$

wherein  $\nu < 0, t > a$ ; for  $\nu > 0$ , we can obtain the corresponding fractional integral definition after doing differential operation to formula (2):

$${}_a D_x^\nu s(x) = {}_a D_x^m ({}_a D_x^{-(m-\nu)} s(x)) \tag{3}$$

wherein  $\nu < 0, t > a$ , this formula is fractional calculus Riemann-Liouville definition, which comes from Cauchy Integral Formula, the conception of common derivative and multiple integral. For distinguishing the representation of fractional integral from fractional differential, the fractional integral Riemann-Liouville definition of signal  $s(x)$  based formula (2) can be expressed as follows:

$$J^\nu s(x) \Big|_{R-L} = \frac{1}{\Gamma(-\nu)} \int_a^x (x-\xi)^{-\nu-1} s(\xi) d\xi, \nu < 0 \tag{4}$$

wherein  $J^\nu$  represents operator of fractional integral with order  $\nu$ ,  $s(x)$  is one-dimensional real signal having duration of  $[a, x]$ .

According to fractional integral Riemann-Liouville definition in formula (4), if duration of signal  $s(x)$  is  $[0, x]$ , following formula can be derived:

$$\begin{aligned}
 J^\nu s(x) \Big|_{R-L} &= \frac{1}{\Gamma(-\nu)} \int_0^x \frac{s(\xi)}{(x-\xi)^{\nu+1}} d\xi \\
 &= \frac{1}{\Gamma(-\nu)} \int_0^x \frac{s(x-\xi)}{\xi^{\nu+1}} d\xi, \nu < 0
 \end{aligned}
 \tag{5}$$

for converting continuous integral into discrete sum so as to can numerically calculate formula (5), integral section  $[0, x]$  is equally divided into  $N$  parts, and when  $N$  is great enough, an approximate formula of following formula can be obtained:

$$J^\nu s(x) \Big|_{R-L} \cong \frac{1}{\Gamma(-\nu)} \sum_{k=0}^{N-1} \int_{kx/N}^{(k+1)x/N} \frac{s(x-\xi)}{\xi^{\nu+1}} d\xi, \nu < 0 \tag{6}$$

So, integral on section  $[0, x]$  is converted into the sum of the integrals of  $N$  sub-sections. In the same manner, when  $N$  is great enough, an approximate formula can be obtained as follows:

$$\begin{aligned}
 \int_{kx/N}^{(k+1)x/N} s(\xi) d\xi &\cong \frac{s\left(\frac{kx}{N}\right) + s\left(\frac{kx+x}{N}\right)}{2} \int_{kx/N}^{(k+1)x/N} d\xi \\
 &= \frac{s\left(\frac{kx}{N}\right) + s\left(\frac{kx+x}{N}\right)}{2} \cdot \frac{x}{N}
 \end{aligned}
 \tag{7}$$

Following formula can be derived from formula (7):

$$\begin{aligned}
 \int_{kx/N}^{(k+1)x/N} \frac{s(x-\xi)}{\xi^{\nu+1}} d\xi &\cong \frac{s\left(x-\frac{kx}{N}\right) + s\left(x-\frac{kx+x}{N}\right)}{2} \int_{kx/N}^{(k+1)x/N} \frac{1}{\xi^{\nu+1}} d\xi \\
 &= \frac{s_k + s_{k+1}}{-2\nu} \cdot \left[ \left(\frac{kx+x}{N}\right)^{-\nu} - \left(\frac{kx}{N}\right)^{-\nu} \right]
 \end{aligned}
 \tag{8}$$

Following formula can be obtained by substituting formula (8) into formula (6):

$$\begin{aligned}
 J^\nu s(x) \Big|_{R-L} &= \frac{1}{\Gamma(-\nu)} \int_a^x (x-\xi)^{-\nu-1} s(\xi) d\xi \Big|_{R-L} \\
 &\cong \frac{1}{\Gamma(-\nu)(-2\nu)} s(x) + \\
 &\frac{1}{\Gamma(-\nu)(-2\nu)} \sum_{k=1}^{n-1} ((k+1)^{-\nu} - (k-1)^{-\nu}) s(x-k) + \\
 &\frac{1}{\Gamma(-\nu)(-2\nu)} (n^{-\nu} - (n-1)^{-\nu}) s(x-n) + \dots, \nu < 0
 \end{aligned}
 \tag{9}$$

wherein, the fractional integral operation of  $s(x)$  is resolved as simple multiplication operation and addition operation such that numerical implementation algorithm for fractional integral of one-dimension signal is derived.

Based on formula (9), when  $k = n \leq N - 1$ , numerical implementation algorithms for fractional integral operations of two-dimension signal  $s(x, y)$  on the negative direction of  $x$  and  $y$  coordinates can be derived as:

$$\begin{aligned}
 J^\nu s(x, y) \Big|_{R-L} &= \frac{1}{\Gamma(-\nu)} \int_a^x (x-\xi)^{-\nu-1} s(\xi, y) d\xi \Big|_{R-L} \\
 &\cong \frac{1}{\Gamma(-\nu)(-2\nu)} s(x, y) + \\
 &\frac{1}{\Gamma(-\nu)(-2\nu)} \sum_{k=1}^{n-1} ((k+1)^{-\nu} - (k-1)^{-\nu}) s(x-k, y) + \\
 &\frac{1}{\Gamma(-\nu)(-2\nu)} (n^{-\nu} - (n-1)^{-\nu}) s(x-n, y) + \dots, \nu < 0
 \end{aligned}
 \tag{10}$$

$$\begin{aligned}
 J^\nu s(x, y) \Big|_{R-L} &= \frac{1}{\Gamma(-\nu)} \int_a^t (y-\xi)^{-\nu-1} s(x, \xi) d\xi \Big|_{R-L} \\
 &\cong \frac{1}{\Gamma(-\nu)(-2\nu)} s(x, y) + \\
 &\frac{1}{\Gamma(-\nu)(-2\nu)} \sum_{k=1}^{n-1} ((k+1)^{-\nu} - (k-1)^{-\nu}) s(x, y-k) + \\
 &\frac{1}{\Gamma(-\nu)(-2\nu)} (n^{-\nu} - (n-1)^{-\nu}) s(x, y-n) + \dots; \nu < 0
 \end{aligned}
 \tag{11}$$

Based on the numerical implementation algorithms for fractional integral operations of two-dimension signal  $s(x, y)$  on the negative direction of  $x$  and  $y$  coordinates in formulae (10) and (11), the sums of first  $n$  terms thereof are taken as the similar coefficient values for fractional integral of  $s(x, y)$  on the negative direction of  $x$  and  $y$  coordinates respectively, shown as formula (12) and (13):

$$\begin{aligned}
 J^\nu s(x, y) \Big|_{R-L} &= \frac{1}{\Gamma(-\nu)} \int_a^t (x-\xi)^{-\nu-1} s(\xi, y) d\xi \Big|_{R-L} \\
 &\cong \frac{1}{\Gamma(-\nu)(-2\nu)} s(x, y) + \frac{2^{-\nu}}{\Gamma(-\nu)(-2\nu)} s(x-1, y) + \\
 &\frac{3^{-\nu} - 1^{-\nu}}{\Gamma(-\nu)(-2\nu)} s(x-2, y) + \frac{4^{-\nu} - 2^{-\nu}}{\Gamma(-\nu)(-2\nu)} s(x-3, y) + \dots + \\
 &\frac{n^{-\nu} - (n-2)^{-\nu}}{\Gamma(-\nu)(-2\nu)} s(x-n+1, y), \nu < 0
 \end{aligned}
 \tag{12}$$

$$\begin{aligned}
 J^\nu s(x, y) \Big|_{R-L} &= \frac{1}{\Gamma(-\nu)} \int_a^t (y-\xi)^{-\nu-1} s(x, \xi) d\xi \Big|_{R-L} \\
 &\cong \frac{1}{\Gamma(-\nu)(-2\nu)} s(x, y) + \frac{2^{-\nu}}{\Gamma(-\nu)(-2\nu)} s(x, y-1) + \\
 &\frac{3^{-\nu} - 1^{-\nu}}{\Gamma(-\nu)(-2\nu)} s(x, y-2) + \frac{4^{-\nu} - 2^{-\nu}}{\Gamma(-\nu)(-2\nu)} s(x, y-3) + \dots + \\
 &\frac{n^{-\nu} - (n-2)^{-\nu}}{\Gamma(-\nu)(-2\nu)} s(x, y-n+1), \nu < 0
 \end{aligned}
 \tag{13}$$

$N$  non-zero values of corresponding terms in formula (12) and (13) are  $\frac{1}{\Gamma(-\nu)(-2\nu)}$ ,  $\frac{2^{-\nu}}{\Gamma(-\nu)(-2\nu)}$ ,  $\frac{3^{-\nu} - 1^{-\nu}}{\Gamma(-\nu)(-2\nu)}$ ,  $\frac{4^{-\nu} - 2^{-\nu}}{\Gamma(-\nu)(-2\nu)}$ ,  $\dots$ ,  $\frac{n^{-\nu} - (n-2)^{-\nu}}{\Gamma(-\nu)(-2\nu)}$ , which are all fractional

integral masks' coefficients according to fractional integral Riemann-Liouville definition. To make the fractional integral mask with rotation invariant, we constructed eight fractional integral masks on direction 135 degrees, 90 degrees, 45 degrees, 0 degrees, 180 degrees, 315 degrees, 270 degrees and 225 degrees respectively. The details of each fractional integral mask are as Fig.1:

$\frac{n^{-\nu} - (n-2)^{-\nu}}{\Gamma(-\nu)(-2\nu)}$	0	⋮	⋮	⋮	⋯	0	$\frac{n^{-\nu} - (n-2)^{-\nu}}{\Gamma(-\nu)(-2\nu)}$	0	⋯
0	⋮	0	0	0	⋯	⋮	⋮	⋮	⋯
⋯	0	$\frac{3^{-\nu} - 1^{-\nu}}{\Gamma(-\nu)(-2\nu)}$	0	0	⋯	0	$\frac{3^{-\nu} - 1^{-\nu}}{\Gamma(-\nu)(-2\nu)}$	0	⋯
⋯	0	0	$\frac{2^{-\nu}}{\Gamma(-\nu)(-2\nu)}$	0	⋯	0	$\frac{2^{-\nu}}{\Gamma(-\nu)(-2\nu)}$	0	⋯
⋯	0	0	0	$\frac{1}{\Gamma(-\nu)(-2\nu)}$	⋯	0	$\frac{1}{\Gamma(-\nu)(-2\nu)}$	0	⋯

(a)

(b)

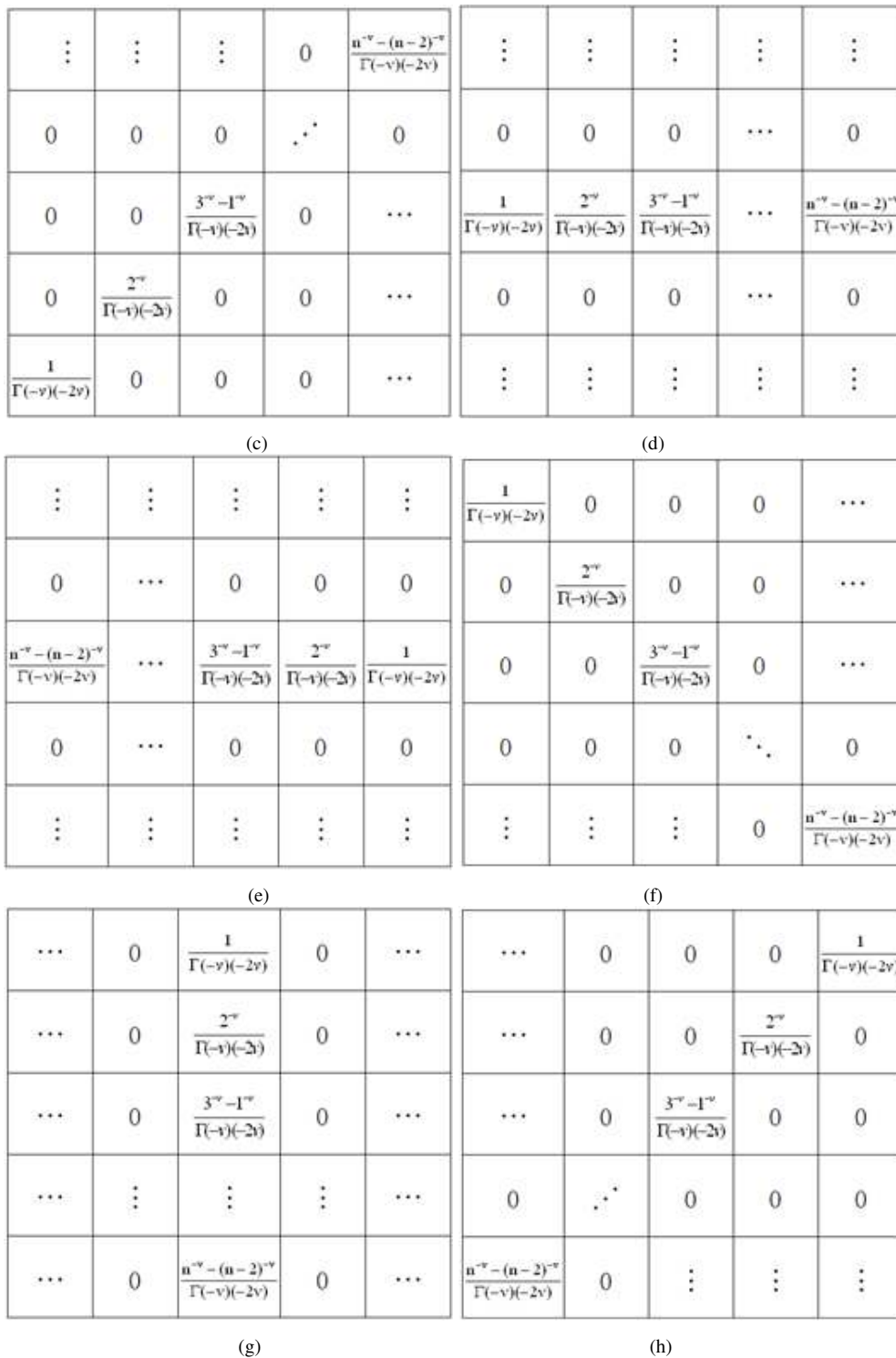


Fig.1 Fractional integral masks on directions of  $135^\circ, 90^\circ, 45^\circ, 0^\circ, 180^\circ, 315^\circ, 270^\circ, 225^\circ$ , and which represented by.

(a):  $FIM_{135^\circ}$ , (b):  $FIM_{90^\circ}$ , (c):  $FIM_{45^\circ}$ , (d):  $FIM_{0^\circ}$ , (e):  $FIM_{180^\circ}$ , (f):  $FIM_{315^\circ}$ , (g):  $FIM_{270^\circ}$ , (h):  $FIM_{225^\circ}$  respectively.

Formula (10) and (11) show that, when  $k \rightarrow n=3$ , FIMs on eight directions is  $3 \times 3$  mask; when  $k \rightarrow n=5$ , it is  $5 \times 5$  mask.  $n$  is usually taken odd number. A natural image becomes into digital image after sampling and quantizing, and the processing for digital image is based on discrete pixels in image. So the FIMs on eight directions filter digital image spatially by moving fractional integral mask

from one pixel to another on image to be filtered. Because the properties of gray image and color image are concerned, they have great differences, the FIIDA uses two different modes to process the gray image and the color image respectively. When processing digital gray image  $S(x, y)$ , we do convolution filter on the above eight directions by using the FIMs on eight directions

respectively. And when processing digital color image, there are correlations among R, G and B components and intensity value is usually limited in [0,255], if we directly do convolution filter on the R, G and B components directly as same as the gray image, the correlations among R, G and B components may be destroyed, which leads to the color distortion. Therefore, we only do convolution filter by FIMs on eight directions for color image on I component in HSI color space.

III. EXPERIMENTS

This section aims at demonstrating the denoising performance of FIIDA. At first, we show the comparison



Fig. 2. Images used in the experiments.

Firstly, we study the performance of the proposed approach using images corrupted with additive, independent Gaussian noise with standard deviation  $\sigma$  5, 10, 15, 20, 25, 35, 50, wherein the fractional integral mask has a size of  $n=3$ , experiment results on Lena is as Fig.3. Fig.3 (a) shows Lena after being corrupted with white Gaussian noise with a standard deviation 15, its PSNR value is 25.55; Fig.3 (b) shows Lena after filtering with Gaussian smoothing filter; Fig.3 (c) shows Lena after filtering with FIIDA, the fractional integral order thereof  $v=-0.001$ ; (d), (e) and (f); (g), (h) and (i) have similar description with (a), (b) and (c) respectively.

to the Gaussian smoothing filter and obtain the qualitative and quantitative analysis for denoising performance of FIIDA. All of the experiments were performed on a set of images (shown in Fig. 2) including those used by Portilla et al [15]. Then, we also quantitatively discuss the relationship between different value of order  $v$  and the performance of FIIDA. The PSNR value in this paper is defined as follows:

$$PSNR = 10\log_{10} \max(f, \hat{f})^2 / MSE \quad (14)$$

$$MSE = \frac{1}{MN} \sum_{i=0}^{M-1} \sum_{j=0}^{N-1} [f(i, j) - \hat{f}(i, j)]^2 \quad (15)$$

From visual sense effect of human eyes, Fig. 3 shows that FIIDA has good denoising performance for Lena corrupted by different level noise; especially when the noise standard deviation is less than 30, FIIDA not only removes the noise well but also reserves the edge and texture details information in the image, in particular for the weak edge; in addition, compared with some algorithms based on TV, anisotropy diffusion, wavelet[16,17,18], because of there is no canonical hypothesis, the FIIDA does not cause the negative effect such as Gibbs vibration or staircase.



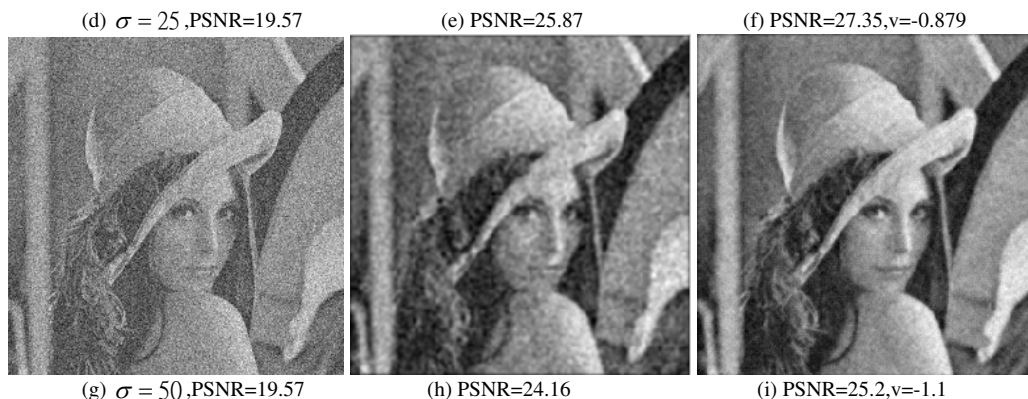


Fig. 3 Denoising results on Lena. Left: Noisy image; Middle: GSF; Right: FIIDA.

Table 1 shows the PSNR values of FIIDA and Gaussian smoothing filter for the test images, wherein NP represents the PSNR values of a noisy image, GSF(s) represents PSNR values of the noisy image after denoised by Gaussian smoothing filter with Gaussian mask having standard deviation s (the size of mask is specified as 5x5), FIIDA(v) represents PSNR value of the image after denoised by FIIDA to noisy image using the FIMs on eight directions with fractional integral order v, and  $\Delta = \text{PSNR}_{\text{FIIDA}} - \text{PSNR}_{\text{GSF}}$ . Data in the table shows that the PSNR values of the image denoised with FIIDA are higher than that with GSF in various extents, and shows that FIIDA's performance is prior to the Gaussian smoothing filter.

IV. CONCLUSIONS

In this paper, we devote to introduce fractional calculus theory into the research field of digital image processing, propose a novel fractional integral image denoising algorithm (FIIDA) which is based on fractional calculus Riemann-Liouville definition, and construct the fractional integral masks on eight directions. Simulation experiments show the availability of FIIDA, that it is prior to the Gaussian smoothing filter, especially when the noise standard deviation is less than 30. Certain aspects of FIIDA need to be studied more carefully.

TABLE I. COMPARISON OF DENOISING PERFORMANCE BETWEEN FIIDA AND GSF

Bacteria.bmp					Peppers.png				
$\sigma$	NP	GSF(s)	FIIDA(v)	$\Delta$	$\sigma$	NP	GSF(s)	FIIDA(v)	$\Delta$
10	27.83	30.57(0.58)	31.3(-0.004)	0.73	10	28.75	29.73(0.52)	30.63(-0.001)	0.9
15	24.94	28.72(0.7)	29.33(-0.36)	0.61	15	24.94	27.97(0.61)	28.47(-0.045)	0.5
20	22.68	27.81(0.86)	28.29(-0.48)	0.48	20	23.14	26.62(0.7)	27.09(-0.28)	0.47
25	20.61	26.59(0.98)	26.99(-0.87)	0.4	25	21.43	25.61(0.8)	26.04(-0.49)	0.43
50	16.6	23.77(1.5)	24.18(-1.3)	0.41	50	17.46	22.69(1.4)	23.25(-1.1)	0.56
Barbara.png					Boat.png				
$\sigma$	NP	GSF(s)	FIIDA(v)	$\Delta$	$\sigma$	NP	GSF(s)	FIIDA(v)	$\Delta$
10	28.48	28.24(0.46)	29.81(-0.001)	0.51	10	28.49	30.73(0.56)	31.2(-0.001)	0.47
15	25.96	27.41(0.53)	27.78(-0.001)	0.37	15	25.63	28.66(0.67)	29.2(-0.053)	0.54
20	23.47	26.02(0.59)	26.26(0.0031)	0.24	20	23.48	27.4(0.78)	27.91(-0.411)	0.51
25	22.12	25.04(0.64)	25.26(-0.219)	0.22	25	21.66	26.46(0.9)	26.97(-0.628)	0.51
50	18.4	22.88(1.08)	22.89(-0.751)	0.31	50	18.1	23.7(1.35)	24.41(-0.991)	0.71

## REFERENCES

- [1] "Special issue: Fractional signal processing and applications", Signal Processing, 2003, 83(11):2285-2286.
- [2] K. B. Oldham, J Spanier. "The Fractional Calculus ". New York: Academic Press, 1974.
- [3] B. Mathieu, P. Melchior, A. Oustaloup. "Fractional differentiation for edge detection". Signal Processing, 2003, 83(11):2421-2432.
- [4] YF Pu, JL Zhou, X Yuan. "Fractional differential mask: a fractional differential-based approach for multiscale texture enhancement". IEEE Transactions on Image Processing, 2010, 19(2):491-511.
- [5] Dennis M., Healy Jr. "Modern Signal Processing ". London: Cambridge University Press, 2004.
- [6] Namias V. "The fractional order Fourier transform and its application to quantum mechanics". Inst Math Appl., 1980, 25:241-265.
- [7] McBride A C, Kerr F H. "On Namias's fractional fourier transform". IMA Journal of Applied Mathematics, 1987, 39: 159-175.
- [8] Y. Huang and B. Suter, "The fractional wave packet transform". Multidimensional System Signal Process, 1998, 9 (4):399-402.
- [9] T. Blu and M. Unser, "The fractional spline wavelet transform: definition and implementation ". Proceedings of the Twenty-Fifth IEEE International Conference on Acoustics, Speech, and Signal Processing (ICASSP'00), vol. I Istanbul, Turkey, 2000, June 5-9:512-515.
- [10] Feyel, D., and de La Pradelle, A.: "Fractional Integrals and Brownian Processes", Potential Analysis, 1996, 10: 273-288.
- [11] Tatom F.B. "The Relationship between Fractional Calculus and Fractals". Fractals, 1995, 3(1):217-229.
- [12] Rocco Andrea, West Bruce. "Fractional calculus and the evolution of fractal phenomena". Physical A, 1999, 265(3,4):535-546.
- [13] E.R.Davies. "Machine Vision: Theory, Algorithms, Practicalities (3rd Ed)". London: Academic Press, 2005.
- [14] B. Ross. "A brief history and exposition of the fundatmental theory of fractional calculus". NewYork: Spring-Verlay, 1975.
- [15] J. Portilla, V. Strela, M.J. Wainwright, and E.P. Simoncelli,. "Image denoising using scale mixtures of gaussians in the wavelet domain ". IEEE Transactions on Image Processing, 2003. 12(11):1338-1351. Nov. 2003.
- [16] Perona, J. Malik, "Scale-space and edge detection using anisotropic diffusion ". IEEE Pattern Analysis and Machine Intelligence, 1990, 12(7): 629-639.
- [17] Rudin LI, Osher S, Fatemi E. "Nonlinear Total Variation Based Noise Removal Algorithms". Physica D, 1992, 60(1):259-268.
- [18] D. L. Donoho, De-noising by soft-thresholding [J], IEEE Transactions on Information Theory, 1995, 41(3):613-627.